Clay minerals and geochemistry of continental shelf sediment around Jeju Island in the northern East China Sea

Jeung su Youn

Department of Earth and Marine Sciences, College of Ocean Science, Jeju National University, Jeju-do 690-756, Korea

제주도 주변해역 대륙붕 퇴적물의 지화학적 조성과 점토광물 연구

윤정수

제주대학교 해양과학대학 해양과학부

Abstract: Geochemical composition and clay minerals of surface and core sediments around off the Jeju Island were analyzed for identification of sediment origins. The clay mineral distribution is mainly controlled by the sediment source and the dominant circulation pattern. Smectite is highly concentrated (>8%) in the northwest near the South Yellow Sea and in the outer-shelf mud patch. It seems to be due to the high supply of smectite transported from China where fine-grained sediments are discharged from modern and ancient Huanghe River. The relatively high abundance of kaolinite are found in northeastern nearshore area and the southwest near Changjiang estuary. It seems to be supplied from Changjiang River and the southwestern Korea rivers. The sediment accumulation rates measured by ^{210}Pb geochronrom mowere 0.20 to 0.54cm/mr or 0.15 to 0.42 g/cm^{2} · mr^{-1} AOJI, with decreasing rates from the west part to the east part, resulting in the supply of fine-grained suspended sediments from the Changjiang and Huanghe Rivers system. The discrimination diagrams clearly show that the sediments around Jeju Island in the northern East China Sea are ultimately sourced from Chinese rivers, especially from the Huanghe River, whereas the sediment in the northeast part might come from Korean rivers and the Jeju Island.

Keywords: clay minerals, accumulation rate, geochemical composition, sediment sources, around off Jeju Island

요 약: 제주도 주변해역에 분포하는 퇴적물의 기원을 밝히기 위해 이곳 표층 및 주상 퇴적물의 지화학적 조성과 점토광물 분석연구를 하였다. 해양에 점토광물의 분포는 주로 퇴적물 공급지와 해양순환 패턴에 의해 지배를 받는다. 스멕타이트는 남황해 북서쪽 지역과 외대륙붕의 니토대 분포지역에 8% 이상의 높은 함량분포를 보이는데, 이는 세립질 부유퇴적물을 많이 함유한 중국의 황하강계로부터 주로 공급되고 있음을 의미한다. 비교적 높은 함량의 고령토는 북동쪽의 연안역과 양자강 하구역에 가까운 남서쪽 지역에 분포하는데 이는 양자강과 한국의 강들로부터 공급된 것으로 보인다. ^{210}Pb 동위원소를 이용한 제주도 주변해역의 퇴적율은 0.20~0.54cm/yr 혹은 0.15~0.42g/cm^{2} · yr^{-1}의 범위를 보였고 서쪽에서 동쪽을 향함에 따라 퇴적율이 점차 감소하는 경향을 보이는데, 이는 황하와 양자강 기원 부유퇴적물이 제주도 주변해역까지 이동되고 있음을 의미한다. 지화학적 구분지수 도표에서 제주도 주변해역은 중국의 강들 중 황하강기원 퇴적물이 주를 이루나 북동쪽 지역은 한국의 강과 제주 기원 퇴적물이 일부 분포하고 있다.

주요어: 점토광물, 퇴적율, 지화학적 조성, 퇴적물 공급지, 제주도 주변해역

1. Introduction

The Yellow and East China Seas form a part of the marginal sea system developed between the north-west Pacific and the Asian continent. One of the most characteristic features of these marginal seas is the input of a large amount of sediments delivered by numerous Chinese and Korean rivers.

The Huanghe(Yellow) and Changjiang (Yangtze) river annually discharge about 8.8×10^8 and 4.3×10^8 tons of suspended sediment into their estuaries respectively, in which part of them can escape the estuaries and deposit in the Yellow and East China Seas (Yang et al., 2003). A number of small rivers draining the Korea peninsular contribute less than 5×10^6 tons suspended sediments to the Yellow Sea annually (Schubel et al., 1984). This riverine particles accumulate in the marine environment forming sedimentary strata, and may also affect biological productivity and the dispersal of particle reactive. It has been postulated that the sediments around Jeju Island (AOJI), located in the southeastern Yellow Sea and northern margin of the East China Sea, are supplied mostly from the Huanghe River and Jeju Island (Milliman et al., 1985a; Yang and Youn, 2007).

The marine environment of the study area, that includes the East China Sea and Yellow Sea, lies within the continental shelf in water less than 150m deep (Fig. 1). The western part of the study area has a broad, almost flat seafloor and gradually steeper gradient of isobathparrom southly stto northeastward average water depth 65m, but the seafloor toward the southeastfloodeeper with maximum depth 150m. The sedimentary processer dn the study area are strongly affectpth 15the complicated h1drodynameraconditions, such as Katoshio Catrent, Yellow Sea Catrent, Jiangsu and Southly stKorea Catrents (Niino and E. Ty, 1961; Lie, 1984). Clay mineral studies in varihe smarine depositional s almoslmoslmoslmoscal sign water havestfply elupedated the provenance, dispersal patterns, transport agents, sedimentary progterses and particle reworking of fine-grained particles (Naedeu and Mowatt, 1983; Hm. and Nelson, 1986; Parkary prhim, 1992; Bhatia; 1983; Cullers et al., 1988;Loring et al;, 1996; Nesbitt et al., 1996), and underalanding the dslmoibutidn and origin of clay mineral arsemblages has provedtto b a e eful tool for3; Cerpreting the net pathway of fine-grained tia; 1983transport (Piper and Slatt, 1977; Karlin, 1980; Naidu et al., 1982).

There has been some previous work on the clay mineralogy and depositional rates of sediment in the East China Sea and adjacent seas (Aoki et al., 1983; Aoki and Oinuma, 1988; Park and Khim, 1992; Nittrouer et al., 1984; DeMaster et al., 1985; Yang and Youn, 2007, Youn et al., 2007). In this study, we present the clay minerals and geochemical composition of sediments collected AOJI in order to identify the sediment origin.

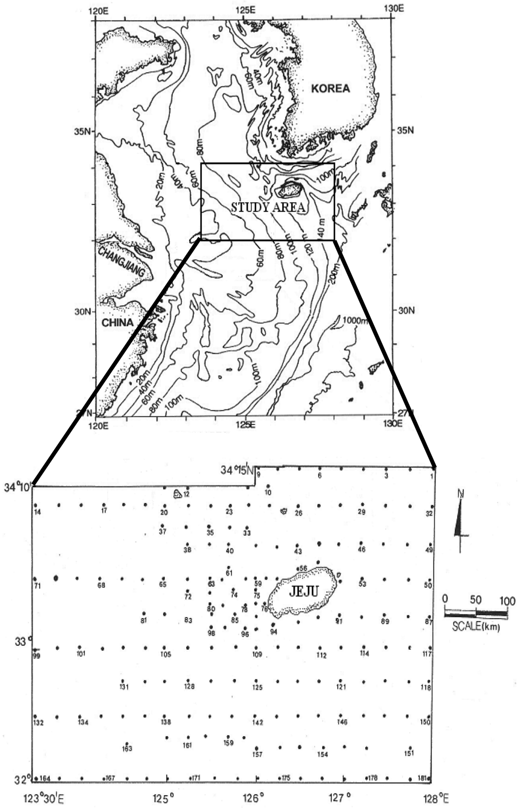

Fig.1 Map showing the study area and the sampling locations with bathymetry in meters.

2. Sample source and methods

A total of 182 sufficient sediment samples were collected from the study area (Fig. 1) between September 1999 and June 2000 with R/V Ara of Cheju National University, the Republic of Korea. In the laboratory, grain-size analyses were performed by standard procedures (Krumbein and Pettijohn, 1938). The sand fraction was analyzed by graded sieving and the silt and clay fraction by pipette techniques. Organic carbon and nitrogen contents in the sediment were analyzed using a CHN Analyzer following the method of Byers et al. (1987). The clay fraction(<2㎛) was smeared on glass and air dried (Gibbs, 1965). Glycolation was affected by vapor-phase exposure for 48hours. All clay specimens were scanned from 2º to 35º2θ at 2º2θ/min on a Shimadzu X-ray diffractometer using Ni-filtered CuK_a radiation. A slow scan (0.25º 2θ/min) between 24º and 26º 2θ was used to differentiate kaolinate from chlorite. Clay minerals were identified from their basal X-ray diffraction peaks according to the criteria outlined by Brindly and Brown (1980). The semi-quantitative determination of relative amounts of major clay minerals was made by measuring the peak area and multiplied by factors of 1, 4, and 2 for smectite, illite and chlorite+kaoline, respectively (Biscaye, 1965). Fine-grained fraction (<62㎛) was used in this study for chemical analysis in order to minimize the grain-size effect on element concentration (Loring and Asmund, 1996; Datta and Subramanian, 1998). The fine fraction was separated from bulk sediments in deionized water by pipetting, dried at 50℃ in a clean oven, and ground in an agate mortar. For element analysis, the powdered sub-samples were digested with HF-HNO_3-$HClO_4$ mixed solution in an airproofed Telflon bomb and then leached with diluted HNO_3 solution. Concentrations of major and some trace elements were measured by an Inductively Coupled Plasma Atomic Emission Spectrometer(ICP-AES, JY58-1) at the Korea Basic Science Institute. The analytic errors monitored by international geostandards are bellows 8%.

For estimating the sediment flux rate of ^{210}Pb into sediment and determining the sedimentation rates six box core samples were analyzed by the radiochemical techniques. Core samples were sectioned at every 1cm interval and each subsample was used for ^{210}Pb analysis. Various methods are available for ^{210}Pb analysis. The one employed is similar to that described by Nittrouer et al. (1979), and depends upon its secular equilibrium with ^{210}Pb. Approximately 3.0g of dried sub-sediment samples, which was passed through a one phi sieve to remove coarse particles, was spiked with a known amount of ^{208}Po tracer. The sample was dissolved in an acid mixture of HNO_3, $HClO_4$, HCl and HF and then taken to dryness. The Po isotopes were digested in 1N HCl and plated onto 1cm^2 silver planchets. The ^{210}Po activated was determined at the Cheju Applied Radioisotope Research Institute (CARDI) by alpha spectrometry.

3. Results and Discussion

3.1. Clay mineral distribution

The sediment in the study area is mainly composed of relict sand, mud, silty clay and sand-silt-clay mixture. The coarse sediments are distributed in the southeast deeper part and around Jeju Island, reported that Holocene transgressive sand sheets. These sand sheets mixed with mud forming sandy mud or muddy sand in the southern Yellow Sea and northern East China Sea are subjected to relatively strong waves and currents (Yang and Sun, 1988). The coarse and fine-grained mixed sediment is mainly distributed in the western part. The small scale mud patches are situated in the southwest off Jeju Island.

In all samples analyzed, illite, chlorite, kaolinite and smectite were identified in varying amounts. The average of individual clay minerals is 67% for illite, 15% for chlorite, 12% for kaolinite, and 6% for smectite(Table 1). Smectite is widely found in soils and shales which have resulted from weathering of mafic rocks and volcanic glasses mainly in poor drainage conditions.

Table 1. Relatives clay mineral abundances of sediment in the Yellow and East China Seas, and adjacent sea and rivers (unit : %).

Region	Smectite	Kaolinite	Chlorite	Illite	Reference
Around off Jeju Island	6(2 - 13)	12(7 - 18)	15(9 - 22)	67(63 - 76)	This study
Huanghe River	23.2	8.4	9.2	59.0	Xu(1983)
Huanghe River	12	10	16	62	Yang e al. (2003)
Ancient Huanghe River	24.0	8.9	8.1	59.0	Xu(1983)
Changjiang River	5.9	14.3	13.1	68.4	Xu(1983)
Changjiang River	6	16	12	66	Yang e al. (2003)
East China Sea	3.0	7.0	28.0	62.0	Aoki et al.(1983)
Central Yellow Sea	13.0	10.0	12.0	67.0	Khim(1988)
Keum River	0.1	17.0	19.3	63.7	Choi(1981)
Yeongsan River	0.1	19.2	16.8	63.9	Kim(1980)

Under low rainfall conditions, the magnesium of mafic rocks remains in the weathered zone and the clay production is mainly smectite (Deer et al., 1971). Smectite content ranges from 2 to 13% in the study area (Table 1). The low content of smectite was also reported by Aoki et al. (1983), being less than 3% in the sediments of the East China Sea. The highest concentration of smectite (<8%) is found in the northwest part near the south Yellow Sea, on west coast of Jeju Island(Stn-41, 42, 49) and the outer-shelf mud deposit (Stn-171, 173; Fig. 2).

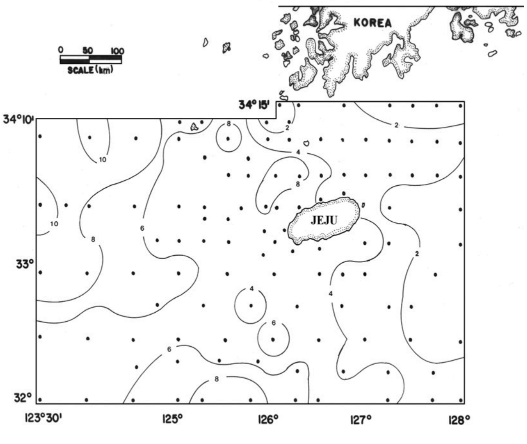

Fig. 2 Distribution pattern(%) of the smectite in surface sediment

The concentration of smectite decreases progressively southeastward from the southern Yellow Sea, suggesting the influence of high smectite input via river runoff from Chinese mainland that received the modern and ancient flow of the Huanghe River. This interpretation is also supported by the comparison in clay mineralogy between the Huanghe and Changjiang rivers sediments (Table 1). The Huanghe River sediment is characterized by the highest average concentration of smectite (12%) with the lowest kaolinate (10%; Yang et al., 2003), whereas the Changjiang River sediments are distinguished by a high amount of kaolinite (16%) and a minor amount of smectite (6%; Yang et al., 2003).

Zhao et al. (1990) reported that suspended sediments from the Huanghe River are dispersed southward, passing the Shandong peninsula, and deposited in the middle of the Yellow Sea. The remaining suspended sediments continue to be transported farther southward by Jiangsu Coastal Current, and finally deposited on the shelf of the East China Sea (Fig. 3). The content of smectite in the outer-shelf mud deposits (Stn-171, 172, 173; Fig. 2) is higher than those in the adjacent areas, which clearly indicates that the resuspended terrigenous materials have been delivered from the Yellow Sea by Jiangsu Coastal Current into this area. Milliman et al. (1985a) also suggested that one potential mechanism for southward transport of Huanghe River-derived mud from the western Yellow Sea is seasonal resuspension during winter storms and advection toward the southeast outer-shelf mud deposits by the dominant circulation, such as the Jiangsu Coastal Current.

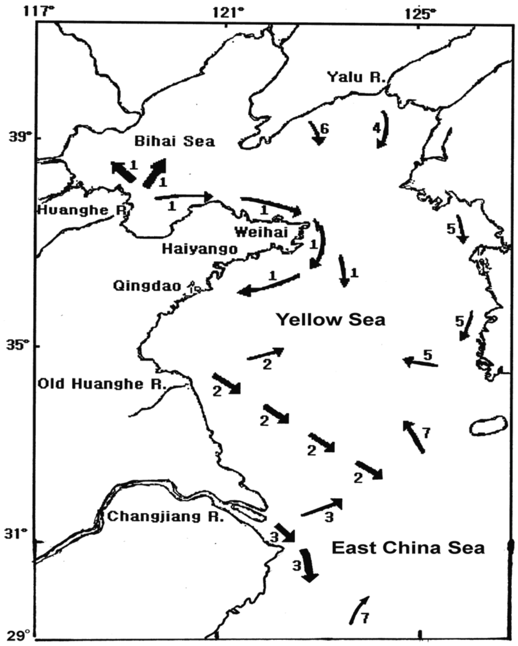

Fig. 3 Transportation trend of the Yellow Sea clays or materials(Zhao et al., 1990). 1. Materials from the Huanghe River; 2. Materials from the old Huanghe River in north Jiangsu; 3. Materials from the Changjiang River; 4. Materials from the Yalu River; 5. Materials from the east coast of the Yellow Sea; 6. Materials from the north coast of the Yellow Sea; 7. Materials from the open sea.

The mud deposits region to the southwest off Jeju Island is a place where the northward flowing Taiwan Warm Current and southward flowing Jiangsu Coastal Currents meet, forming a cyclonic gyre that may have deposited muddy sediment at the center (Beardsley et al., 1985). The concentration of smectite (<8%) in the northwest coast of Jeju Island may be attributed to the relatively large supply of smectite from the volcanic glasses of Jeju Island (Young et al., 2006). Kaolinite is a common weathering product of feldspar, under the intense chemical weathering condition, Muscovite, k-feldspar and plagioclase provide the alumina and silica necessary forming kaolinite (Grim and Loughman, 1962; Griffin et al., 1968).

Fig. 4 shows the kaolinite distribution AOJI, varying from 7 to 18%. The high concentration areas are southwest off Changjiang river estuary, in the northeast nearshore area of Korean peninsular and the west coast of Jeju Island (Fig. 4). More than 12% high concentration of kaolinite occurs southwest offshore near Changjiang River estuary and decreases gradually northeastward, resulting from the supplies of fine-grained kaolinite-rich particles from the Changjiang River. The Changjing River deposits have been known to be enriched with kaolinite (average at 14,3%), compared to the Huanghe River sediments (average at 8.4%; Xu, 1983). According to Yang and Millimam (1983), the drainage area the Chagjiang River is located in a warm and humid climate zone, where chemical erosion is intensive, and mostly with acidic soils of Al content and a relatively high concentration of kaolinite in the south coast of the Korean peninsular that seems to be transported from the southern Yellow Sea and the South Sea of Korea. The nearshore of the South Sea of Korea consists of more than 20% kaolinite content in a wide range of lithofacies from the adjacent land (Park and Han, 1985).

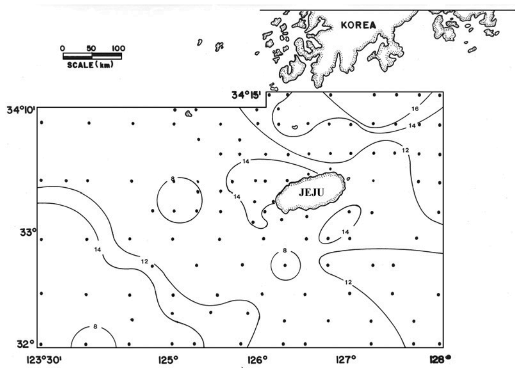

Fig 4. Distribution pattern(%) of the kolinite in surface sediment

The relative abundance of clay minerals in the study area and adjacent regions are summarized in Table 1, which may help explain and distinguish the sources of the sediments in the study area. The Huanghe River in China supplies during ancient and modern times a relatively high concentration of smectite, with less amounts of kaolinite and illite, while the Changjiang River clay suites are distinguished by a high concentration of kaolinite and a minor amount of smectite. In the Keum and Yeongsan Rivers in Korea, smectite is nearly absent, but kaolinite and chlorite are dominant (Table 1). This implies that smectite in the study area might not come from the Korean peninsula. Instead, it seems to have been being controlled mainly by the Huanghe River system since very ancient times. The clay minerals AOJI are characterized by abundant illite (67%), chlorite (15%) and lack of smectite (6%). These values are similar to those of the East China Sea sediments. Therefore, we suggest that the clay minerals in the study area are a mixture of clays derived predominantly from modern and ancient Huanghe River, the Changjiang River, and to a smaller extent from the south Korean peninsular.

3.2. ^{210}Pb profiles and accumulation rates of cores

Oceanographers often use ^{210}Pb to construct chronologies of sediment cores. These unstable isotopes have a relatively short-half life of 22.3 years, which makes them ideal to estimate the sedimentation rate of deposited marine sediment over the past 100 years (Koide et al., 1973; Nittrouer et al., 1979). Figs. 5 and 6 show the vertical profiles of total and excess ^{210}Pb ($^{210}Pb_{ex}$) activities for 6 sediment cores. Most of the cores exhibit a typical ^{210}Pb profile characterized by three distinct zones: a surface middle layer (SML) with uniform activity, a middle inclined zone with exponential radioactive decay, and a lower background zone of constant low activity. In most of the ^{210}Pb profiles, the SML, a layer

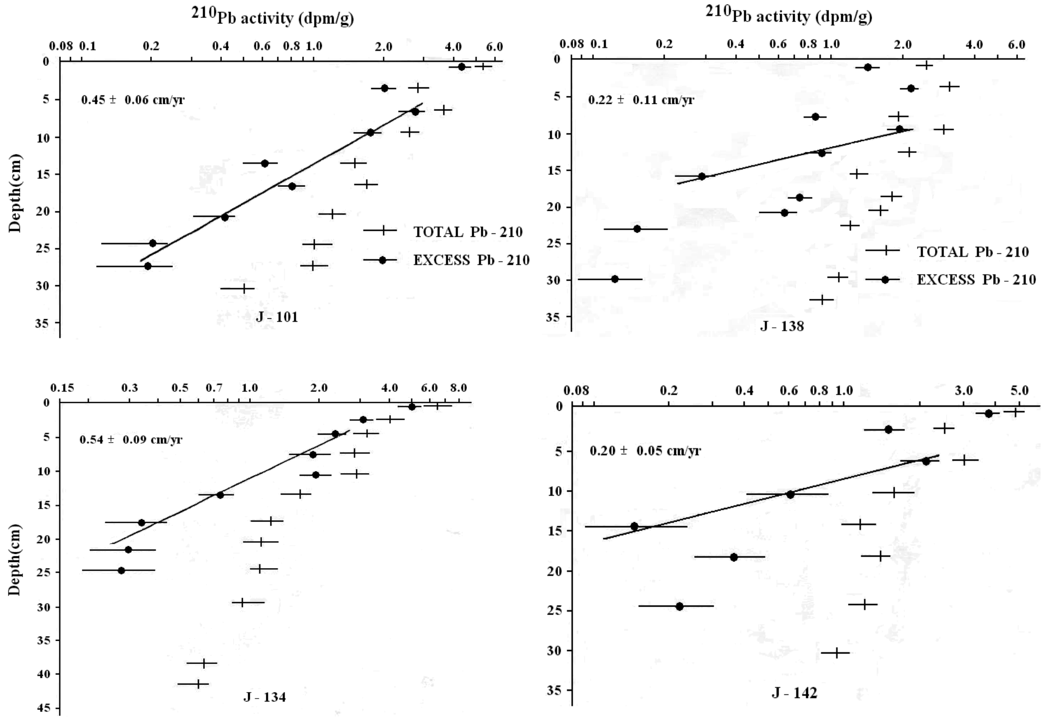

Fig 5. Depth profiles of 210Pb activity from cores J-101, J-134, J-138 and J-142 in the study area.

Table 2. The 210Pb dating results from the core samples around Jeju Island

Core No.	Number of lineal segments (cm)	Linear range (cm)	Surface ^{210}Pb activity (dpm/g)	Sedimmtation rates (cm/yr)	Sediment material flux $(g/cm^2 \cdot yr^{-1})$	^{210}Pb sedimentation flux $(dpm/cm^2 \cdot y^{r-1})$
J-59	13	48	3.07	0.21	0.16	0.82
J-91	12	45	4.15	0.44	0.34	1.44
J-101	10	41	2.78	0.45	0.35	1.48
J-134	12	42	2.98	0.54	0.42	2.31
J-138	11	40	1.79	0.22	0.17	0.36
J-142	8	4	1.84	0.20	0.15	0.57

of relatively uniform activity, was observed in the uppermost 5～8cm of the cores. Generally, this layer probably results from strong physical and/or biological mixing. Sediment accumulation rates were determined from $^{210}Pb_{ex}$ by subtracting the supported levels of ^{210}Pb activity from the total ^{210}Pb measured. The ^{210}Pb supported activity was determined in a few section core samples using the ^{222}Rn emanation method (Lucas, 1975; Nittrouer et al., 1979). The amount of excess ^{210}Pb in samples was calculated by extracting the background ^{226}Ra activity from the total ^{210}Pb activity. ^{210}Pb activities are plotted versus depth in sediment cores in Figs. 5 and 6. The crosses represent the total ^{210}Pb activity and the closed circles represent the excess ^{210}Pb activity with the same point after the background is subtracted.

The sediment accumulation rates obtained using the simplied equation of Nittrouer et al. (1979) in the study area range from 0.20 to 0.54cm/yr or 0.15 to $0.42 g/cm^2 \cdot yr^{-1}$. The sedimentation rates from the cores J-101 and J-134 in the southwest offshore region near the Changjiang River estuary range from 0.45 to 0.54 cm/yr. This may have derived from the high input of suspended sediments in river runoff from the China side, such as the Changjiang and Huanghe Rivers. According to Zheng and Klema (1982), the Changjiang river fresh water, during years of high flood flows, is directed to the northeast and spreads near the southwest off Jeju Island. The sediment cores J-138 and J-142 from the outer-shelf mud deposits in the southwest off Jeju Island, the estimates of sediment accumulation rates range from

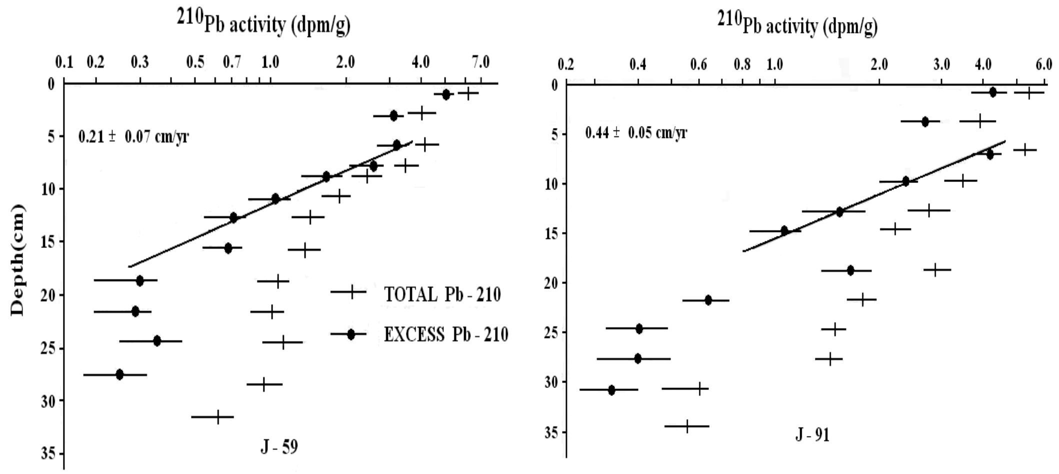

Fig. 6 Depth profile of 210Pb activity from cores J-59, J- 91 in the study area.

0.20 to 0.22 cm/yr and were much lower than the above two samples. This may have resulted from the weakened sediment transported. According to Milliman et al. (1985b), the outer-shelf mud deposits were derived from the ancient Huanghe River delta off the northern Jiangsu coast and where the Huanghe River induced mud is presently accumulated, and also where a maximum sediment accumulation rate is 0.3cm/yr (DeMaster et al., 1985).

The sedimentation rates from cores J-59 and I-91 around the coast of Jeju Island range from 0.21 to 0.44cm/yr (Fig. 6), indicating that terrigenous materials from Jeju Island are supplied to this environment. Table 2 presents a summary of the number and range of segments included in the surficial ^{210}Pb activity, sediment material flux, and ^{210}Pb sedimentation flux. The surficial ^{210}Pb activity values range from 1.79 to 4.15dpm/g. The muddy sediment cores around the coast of Jeju Island have high surface ^{210}Pb activity compared to the entire cores. Here, it is thought to more easily absorbed ^{210}Pb than the other sediments. The ^{210}Pb sedimentation fluxes and the sediment material fluxes AOJI cores range from 0.36 to 2.31dpm/cm^2·yr^{-1} and 0.15 to 0.42g/cm^2·yr^{-1}, respectively. The high sediment material fluxes (0.42g/cm^2·yr^{-1}) in the case of the core J-131 may be related to the high ^{210}Pb influx with terrigenous suspended materials from the Changjiang River estuary and also the delta off the northern Jiangsu coast. The low sediment accumulation rates range from 0.15 to 0.17g/cm^2·yr^{-1} measured in the southwest offshore mud deposit cores J-138 and J-142 (Table 2), which is in good agreement with a decrease in accumulation rate with increasing water depth. This is likely the result of progressive seaward depletion of influx and reworking of detrial materials.

3.3. Elemental concentration and geochemical signature

Mean grain size and elemental concentrations around the Jeju Island (AOJI) sediments are presented in Table 3, with averaged elemental concentrations from the Changjiang, Huasnghe, Keum rivers and upper continental crust shales(UCC) listed for comparisons. The element content of AOJI sediments are low compared to UCC (Taylor and McLennan, 1985; Table 3) This could be due to provenance, strong chemical weathering of the source rock compared to continentally derived shales. Comparing the AOJI sediments and Chinese (Changhjiang and Huanghe) and Korean (Keum) river sediments, the sediments from the AOJI are characterized by a relatively higher concentration of Ca and Sr mainly because of the abundant shell fragments in the sediment samples. The Changjiang sediments are high in Fe, Mg and Ti, the Huanghe sediments in Na, Ca, and Sr, and Keum sediments in K, Ba and Al (Table 3). All these elements may therefore potentially be used as geochemical signatures of the originating river system.

The present study is to induce some quantitative indices that can be used in the discrimination of provenance of sediments in the AOJI. It is therefore to fine out some useful numerical expressions using 5 signature elements, i.e., Al, Fe, Ca, Mg, and K, which can be easily calculated from major element composition data and effectively distinguish the 3 major source river system (Table 3). The first index is (Al+Fe)/(Ca+Mg+K), representing the element concentration ratio of environmentally immobile over mobile elements and includes all the 5 signature elements derived from this study. The study area sediment samples could be clearly discriminated by this index. The second index is (Ca-Fe)/Al, which is particularly sensitive in discriminating the Huanghe-derived sediments that show the highest values of Ca and lowest values of Al. The third index is (Ca-Mg)/K, which uses the relatively labile elements among the signatures of three end-member rivers. Paired diagrams of (Al+Fe)/(Ca+Mg+K) vs. (Ca-Fe)/Al, (Al+Fe)/(Ca+Mg+K) vs. (Ca-Mg)/K, and (Ca-Fe)/Al vs. (Ca-Mg)/K clearly show that the AOJI sediments cluster into two type (Fig. 7). Most of the study area sediment samples are located between the Huanghe and Changjiang sediments averages, especially more approx-

Table 3. Elements concentration around the Jeju Island shelf sediments in comparison to Huanghe(HURS), Chanjiang , Keum(KUMS) river sediments and UCC(unit:*in wt.%, Mn, Ba, Sr, and Rb; μg/g)

St.	Al*	Fe*	Ca*	K*	Na*	Mg*	Ti*	Mn	Ba	Sr	Rb	TOC*	CaCO3*	Mz
14	7.2	2.5	3.7	2.6	2.1	1.3	0.36	455	538	156	101	1.04	3.02	7.23
16	7.6	3.3	3.5	2.6	1.8	1.3	0.39	697	442	175	98.6	0.61	4.17	6.37
18	6.2	3.6	4.1	2.5	2.6	0.9	0.28	378	414	230	134	0.29	4.25	4.57
20	7.3	3.8	4.6	2.6	2.6	1.1	0.43	650	415	209	98.4	0.26	4.66	5.45
22	7.2	2.9	3.8	2.2	1.3	1.2	0.33	480	385	220	72.2	0.91	4.83	8.07
24	5.4	2.5	5.2	1.9	1.9	0.9	0.25	420	410	320	81.2	0.59	6.75	4.34
26	7	2.6	5.6	2.8	1.2	1	0.32	593	473	282	105	0.68	6.09	5.48
28	5.8	2.7	5	2.2	1.6	0.8	0.27	318	471	269	133	0.49	6.73	4.1
54	5.1	2.5	5.6	1.8	1.5	0.7	0.2	308	321	325	95.4	0.32	8.22	3.12
56	5.3	2.4	4.7	1.4	1.3	1.1	0.23	462	340	273	87.1	0.46	6.9	4.2
59	5.2	2.7	5.5	1.7	1.1	1.3	0.21	416	324	212	70.2	0.39	6.7	4.59
63	6.6	2.7	4.3	2.5	2.6	1.2	0.29	397	205	312	122	0.56	4.01	5.78
65	6.4	2.8	4.7	2.4	2.4	1.1	0.3	411	229	259	117	0.32	5.08	5.32
67	7.3	3.1	4.5	2.6	2.7	1.3	0.33	447	219	223	132	0.66	2.67	6.67
69	7.5	3.5	4.8	2.6	2.8	1.3	0.36	459	236	204	129	0.62	2.58	7.33
71	7.4	3.2	4.2	2.2	1.6	1.4	0.4	519	387	150	101	0.98	2.17	6.1
99	7.4	3	3.3	2.1	1.5	1.3	0.44	614	363	156	96.3	0.95	2.31	5.73
101	6.7	3.1	3.7	2	1.5	1.2	0.37	380	418	182	98.6	1.07	1.92	6.93
103	5.8	2.6	3.8	2.4	1.6	1.1	0.34	416	474	178	105	0.89	2.98	5.43
105	6.4	3.3	3.1	2.4	1.7	1.4	0.33	524	476	260	120	0.54	4.25	6.65
107	6.9	3.1	3.7	2.5	2	1.3	0.26	450	453	230	121	0.27	6.16	4.73
109	6.5	2.8	4.3	2.1	2	0.9	0.27	380	446	248	119	0.36	6.33	2.92
111	6.6	3.4	4	2.5	1.8	1.2	0.28	500	326	230	79.5	0.56	7.3	5.3
113	6.8	2.4	4.5	2.2	1.7	1.3	0.2	254	448	330	65	0.65	7.07	4.7
132	6.3	2.9	3.6	2.3	1.6	1.5	0.36	525	392	175	82.2	0.51	2.85	3.93
134	7.2	4.1	3.2	2.4	1.5	1.4	0.5	650	419	200	99.7	0.5	2.3	5.13
136	6.2	3.2	3.1	2.2	1.7	1.1	0.38	480	446	180	97.7	0.38	2.92	6.27
138	6.3	3.9	3.1	2.5	1.9	1.4	0.45	598	437	190	136	0.97	3.75	7.47

Huanghe, Changjiang(CHRS) and Keum rivers sediment(Yang et al., 2004); Average upper continental crust (UCC: Taylor and McLnnan, 1981); Mz is mean grain size with unit of ϕ, TOC: total organic carbon.

Table 3. (Continued)

St.	Al*	Fe*	Ca*	K*	Na*	Mg*	Ti*	Mn	Ba	Sr	Rb	TOC*	CaCO3*	Mz
142	7	3.1	5.4	2.3	1.8	1.3	0.2	600	414	210	88.4	0.71	2.93	6.33
144	7.9	3.7	6.8	2.4	2.3	1.7	0.4	770	398	280	85.6	0.64	6.02	7
146	7.2	2.6	4.6	2.3	1.7	1.2	0.3	287	409	250	64.9	0.74	7.14	3.93
164	5.8	2.7	3.1	2	1.8	1.1	0.4	440	445	181	64.7	0.14	3.25	2.43
166	6.2	3.2	3.4	2.1	1.9	1.2	0.4	560	415	210	66.2	0.34	3.18	3.5
168	6.8	3.5	3.1	2.7	2.2	1.4	0.5	404	617	178	90.2	0.57	3.08	4.73
170	5.4	3	3.2	2.4	1.5	1	0.5	519	414	163	82.7	0.37	3.95	4.67
172	8.2	4.1	4.6	2.6	1.8	1.7	0.4	560	422	175	95.9	0.83	2.77	7.2
174	8	4.2	4.8	2.8	1.9	1.8	0.4	650	429	200	104	0.85	2.25	7.2
176	5.7	2.9	3.7	2.1	1.9	1.3	0.3	430	383	330	86.4	0.5	4.5	6
178	6.1	2.4	4.4	2.3	1.6	1.5	0.3	302	408	367	78.1	0.71	5.91	3.5
Avg	6.5	3	4.1	2.3	1.8	1.2	0.3	468	392	223	95.1	0.58	4.45	5.26
HURS	5.55	2.52	4.01	1.9	1.65	1.15	0.4	700	453	207	81.7	0.25	9.7	5.1
CHRS	7.02	4.28	3.18	2.06	0.91	1.64	0.6	1000	454	146	113	0.82	6.5	6.3
KUMS	7.36	3.09	0.02	2.25	1.45	0.92	0.4	586	492	149	132	0.64	0.26	7.3
UCC	8.04	3.5	3	2.83	2.89	1.33	0.4	600	550	350	112			

Huanghe, Changjiang and Keum rivers sediment(Yang et al., 2004), Average upper continental crust(Taylor and McLnnan, 1981), Mz is mean grain size with unit of ϕ, TOC: total organic carbon.

imate to the Huanghe cluster, but the sediments in the southwest part of the study area (Stns. 105, 134, 138, 168) are closely plotted with Changjiang River sediments. In contrast, sediment samples off the north-eastern Jeju Island coast (24, 26, 28, 54, 56, 59) show the highest values than those of the river sediments and other regions, which are supplied mostly from Jeju Island in a Quaternary shield volcano, composed of hawiite, alkaline basalt, megearite and trachyte (Park and Kwon, 1993). It is intuitively considered that the sediments in the vicinity of Jeju Island may be at least partly locally derived. Consequently, these discrimination diagrams suggest that the surface sediments AOJI are originated from diverse sources including the Huanghe and Changjiang rivers and Jeju Island.

4. Conclusions

Coarse sediment is distributed in the southeast deeper part of the East China Sea and Yellow Sea, whereas fine-grained sediments are mainly distributed in the western region. Smectite is highly concentrated in the northwest area of the sea and west coast of Jeju Island. It seems to be mainly controlled by the Huanghe River system, and the result of supplies of smectite altered volcanic materials from Jeju Island. More than 12% of a high concentration of kaolinite occurs in the southwest offshore region and in the northeast near the Korean peninsular. It can be supplied by the Changjiang River and influenced by lithofacies on adjacent land to the South Sea of Korea. The sedimentation rates in the southwest part near the Changjiang River estuary, range

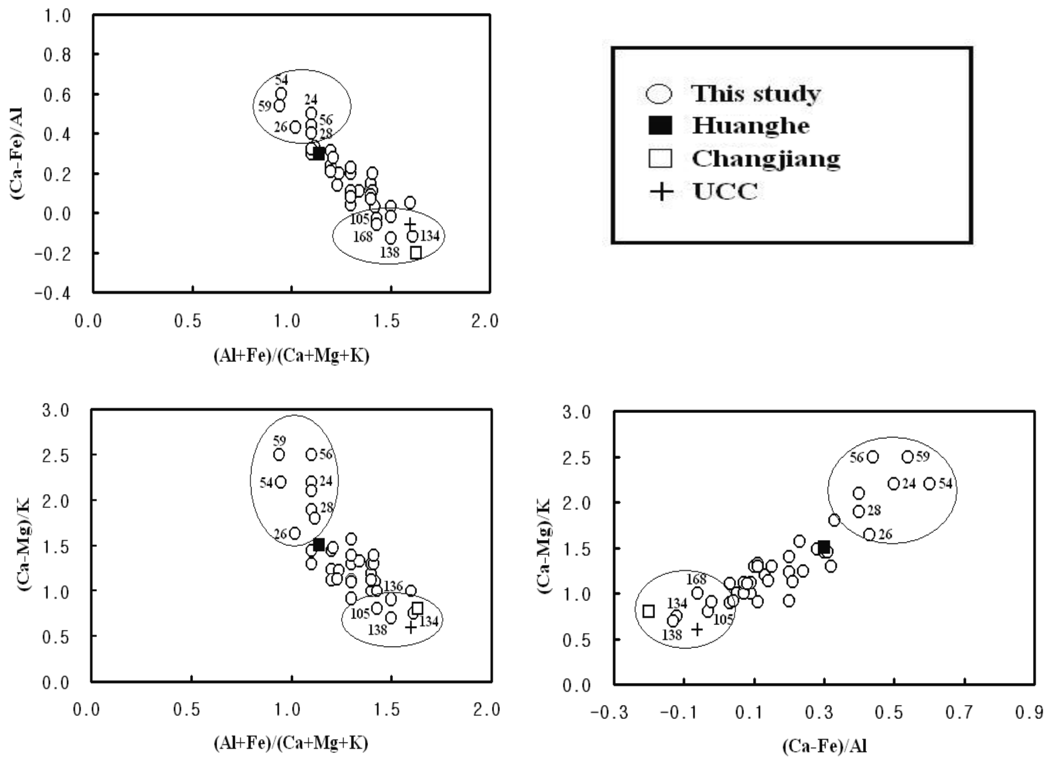

Fig.7 Comparison of the geochemical indices of (Al+Fe)/(Ca+Mg+K), (Ca-Fe)/Al, and (Ca-Mg)/K. The value of UCC (by Taylor and McLennan,1985), and the river sediments(Changjiang and Huanghe) are sourced from Yang et al. (2004).

from 0.45 to 0.54cm/yr, while the accumulation rates in the outer-shelf mud deposits range from 0.20 to 0.22cm/yr which is lower than in the western region. This might be the result of the weakened sediment transported from the China side. Based on the differences in 5 major element compositions of sediment samples, the riverine sediments can be distinguished by 3 geochemical indices of (Al+Fe)/(Ca+Mg+K), (Ca-Fe)/Al, and (Ca-Mg)/K. Applications of geochemical indices on the sediments around Jeju Island show a blended feature of the Huanghe and Changjiang river sediments.

Acknowledgements

The authors would like to thank Mr. T. J. Kim and Mr. S. J. Song at Applied Radioisotope Research Institute for their helpful guidance in the use of isotopic facilities. Thanks extend to Mr. S. H. Lee and Mr. S. Y. Bae for sampling process and analytic work.

References

Aoki, S., Oinuma, K., 1988. The distribution of clay minerals in surface sediments of the Okhotsk Sea to the South China Sea along the Asiatic Continent. Clay Science 7, 73-82.

Aoki, S.K., Oinuma, K., Matsuike, K., 1983. Clay mineral composition in surface sediments and the concentration of suspended matter of the East China Sea. In: Sedimentation on the Continental Shelf with Special Reference to the East China Sea 2, China Ocean Press, Beijing, pp. 440-449.

Brindley, G. W., Brown(Ed), G., 1980. Crystal structures and clay minerals and their X-ray identification. London Mineralogical Society Monograph 5, pp. 495-497.

Biscaye, P.E., 1965. Mineralogy and sedimentation of recent deep-sea clays in the Atlantic Ocean and adjacent seas and ocean. Geological Society of America Bulletin 76, 803-832.

Bhatia, M.R., 1985. Composition and classification of Paleozoic flysch mudrocks of eastern Australia: Implications in provenance and tectonic setting interpretation. Sedimentary Geology 41, 249-268.

Beardsley, R.C., Limeburner, R., Yu, H., Cannon, G.A., 1985. Discharge of the Changjiang(Yangtze River) into the East China Sea. Continental Shelf Research 4, 57-76.

Byers,S.C., Mill, E.L., Stewart, P.I., 1987. A comparison of method for determining organic carbon in marine sediments with suggestion for a standard method. Hydrobiology 58, 43-47.

Culler, R.L., Basu, A., Suttner, L.J., 1988. Geochemical signature of provenance in sand-size material in soils and stream sediment near the Tobacco Toot Batholith, Montana, USA. Chemical Geology 70, 335-348.

DeMastwr, D.J., Mckee, B.A., Nittrouer, C.A., Oian, J., Cheng, G., 1985. Rates of sediment accumulation and particle reworking based on radiochemical measurement from continental shelf deposit in the East China Sea. Continental Shelf Research 4, 143-158.

Deer, W.A., Howie, R.A., Zussaman, J., 1971. Clay minerals, A introduction to the rock forming minerals. Longman Group Limited London Publication, pp. 250-274.

Griffin, J.J., Windom, H., Goldberg, E.D., 1968. The distribution of clay minerals in the world oceans. Deep Sea Research 15, .433-459.

Gibbs, R.J., 1965. Error due to segregation in quantitative clay mineral X-ray diffraction mounting technique. American Mineralogist 50, 741-751.

Grim, R.E., Loughman, F.C., 1962. Clay minerals in sediments from Sydney Harbor in Australia. Journal of Sedimentary Petrology 32, 240-248.

Hume, T.M., Nelson, C.S., 1986. Distribution and origin of clay minerals in the surficial shelf sediments, western North Island, New Zealand. Marine Geology 69, 289-308.

Krumbein, W.C., Pettijohn, F.J., 1938. Manual of sedimentary petrography, Appleton Century Crofts, York, N. Y., pp. 549-552.

Karlin, R., 1980. Sediment sources and clay mineral distribution off the Oregon coast. Journal of Sedimentary Petrology 50, 543-560.

Koide, M. Bruland, K.W., Goldberg, E.D., 1973. ^{228}Th/^{232}Th and ^{210}Pb geochronologies in marine and lake sediments. Geochim. Cosmochima. Act 37, 1171-1187.

Lie, H.J., 1984. A note on water mass and general circulation in the Yellow Sea(Huanghe). Journal Korean Society of Oceanography 19, 187-194.

Loring, D.H., Asmund, G.., 1996. Geochemical factors controlling accumulation of major and trace elements in Greenland coastal fjord sediments. Environmental Geology 28, 1-11.

Lucas, H.F., 1975. Improved low-level alpha sintillation counter for radon. Review Science Inster. 28, 680-683.

Milliman, J.D., Beardsley, R.C., Yang, J.S., Limebruner, R., 1985a. Modern Huanghe River mud on the outer shelf of the East China Sea: Identification and potential transport mechanisms, Continental Shelf Research 4, 175-188.

Milliman, J.D., Shen, H.T., Yang, Z.S., Meade, R.H., 1985b, Transport and deposition of river sediment in the Changjiang estuary and adjacent continental shelf. Continental Shelf Research 4, 37-45.

Niio, H., Emery, K.O., 1961. Sediment of shallow portion of East China Sea and South China Sea. Geological Society of America Bulletin 72, 731-762.

Naidu, A.S., Mowatt, T.C., 1983. Sources and dispersal patterns of clay minerals in surface sediments from the continental shelf areas off Alaska. Geological Society of American Bulletin 94, 841-854.

Naidu, A.S., Creager J.S., Mowatt, T.C., 1982. Clay mineral disperal in the north Bering and Chukchi Sea. Marine Geology 47, 1-15.

Nittrouer, C.A., Sternberg, R.W., Carpenter, R., Bennett, J.T., 1979. The use of ^{210}Pb geochronology as a sedimentological tool: Application to the Washington continental shelf. Marine Geology 31, 279-316.

Nittrouer, C.A., DeNaster, D.J., Mckee, B.A., 1984. Fine-scale stratigraphy in proximal and distal deposits of sediment dispersal systems in the East China Sea. Marine Geology 61, 13-24.

Nesbitt, H.W., Yuong, G..M., McLennan, S.M., Keays, R.R., 1996. Effects of chemical weathering and sorting on the petrogenesis of siliciclastic sediments, with implication for provenance studies, Journal of Geology 104, 525-542.

Park, Y.A., Khim, B.K., 1992. Origin and dispersal of recent clay minerals in the Yellow Sea. Marine Geology 104, 205-213.

Piper, D.J., Slatt, R.M., 1977. Late Quaternary clay mineral distribution on the eastern continental margin of Canada. Geological Society of American Bulletin 88, 267-272.

Park, B.K., Han, S.J., 1985. The distribution of clay minerals in recent sediments of the Korea strait. Sedimentary Geology 41, 173-184.

Schubel, J.R., Shen, H.T., Park, M.J., 1984. A comparison of some characteristic sedimentation progress of estuaries entering the Yellow Sea. In: Proceeding of Korea – US Seminar and Workshop, Marine Geology and Physical Processes of the Yellow Sea, pp. 286-308.

Xu, D., 1983. Mud sedimentation on the East China Sea shelf. In; Sedimentation on the Continental Shelf with Special Reference to the East China Sea 2, China Ocean Presson tijing, pp.506-516.

Yang, Y.Y., Jung, H.S., Lim, D.I , Li, C. X., 2003. A review on the provenance discrimination of sdiment in the Yellow Sea. Earth-Science Reviews 63, 93-120.

Yang, S.Y., Youn, J.S., 2007. Geochemical compositions and provenance discrimination of the central south Yellow Sea sediments. Marine Geology 243, 229-241.

Yang, C.S., Sun, J.S., 1988. Tidal sand ridges on the East China Sea shelf. Tide-Influence Sedimentary Environments and Facies 12, 23-38.

Youn, J.S., Byun, J.C., Lee, S.H., 2006. Sedimentary strata and clay mineralogy of continental shelf mud deposits in the East China Sea. International Journal of Oceans and Oceanography 11, 183-194.

Youn, J.S., Yang, S. Y., Park, Y.A., 2007. Clay mineranls and geochemistry of the bottom sediments in the northwestern East China Sea, Chinese Journal of Oceanology and Limnology 25, 235-246.

Yang, Z., Milliman, J.D., 1983. Fine-grained sediment sources of East China Sea. In; Sedimentation on the Continental Shelf with Special Reference to the East China Sea 2, China Ocean Press, Beijing, pp.405-415.

Zhao, Y.Y., Qin, Z.Y., Li, F.G., Chen, Y.W., 1990. On the sources and genesis of the mud in the central area of the South Yellow Sea. Chinese Journal of Oceanology Limonology 8, 66-73.

Zheng, Q.A., Klema, V., 1982. Determination of winter temperature patterns, and surface currents in the Yellow Sea and East China Sea from satellite imagery. Remote Sensing Environment 12, 201-208.